ARTICLE NO. 78-197R

C 80-014

Noise Transmission into a Light Aircraft

00004
00013
00023

R. Vaicaitis*
Columbia University, New York, N.Y.

An analytical study on noise transmission into a cabin of a twin-engine G/A aircraft is presented. The solution of the governing acoustic-structural equations of motion is developed utilizing modal expansions and a Galerkin-type procedure. The exterior noise pressure inputs are taken from available experimental data. A direct comparison between theory and experiments on cabin noise levels is given. Interior noise reduction by stiffening, mass addition, and damping treatments is investigated. It is shown that a combination of added mass and damping could significantly reduce interior noise levels for this aircraft.

Nomenclature

a	= cabin dimension (see Fig. 2)
a_x,a_y	= panel dimensions (see Fig. 2)
a_0,b_0	= distances from x and y axes, respectively (see Fig. 2)
A_{ij}	= defined by Eq. (9)
b	= cabin dimension (see Fig. 2)
B_{ijk}	= acoustic pressure modal coefficients
c	= speed of sound in the cabin
d	= cabin dimension (see Fig. 2)
D	= $Eh^3/12(1-\nu^2)$, panel stiffness
e_{ij},e_k	= defined by Eqs. (13) and (21), respectively
E	= modulus of elasticity of the elastic panels
E_{ij}	= defined by Eq. (12)
E_p	= modulus of elasticity of window Plexiglass
E_2	= modulus of damping tape
f	= frequency, Hz
F_{ijk}	= defined by Eq. (20)
G	= shear modulus of the viscoelastic sandwich core
G_{ij}	= defined by Eq. (11)
h	= plate thickness
h_T	= damping tape thickness
H_{ijk}	= acoustic frequency response function defined by Eq. (19)
H_{mn}	= panel frequency response function defined by Eq. (27)
i,j,k,m,n	= indices
i	= imaginary unit $(-1)^{1/2}$
$\bar{L}_{ijmn}$	= defined by Eq. (34)
m_s	= panel mass
M_{mn}	= generalized mass defined by Eq. (30)
M_x	= number of added stiffeners perpendicular to x coordinate
M_y	= number of added stiffeners perpendicular to y coordinate
OASPL	= overall sound pressure level, dB
$p(x,y,z,t)$	= acoustic pressure
$p^r(x,y,t)$	= external pressure
P^c_{mn}	= generalized cavity force
P^r_{mn}	= generalized external force
q_{mn}	= generalized coordinates
Q	= forcing term in Eq. (1)
S_I	= external pressure spectral density
SPL	= sound pressure level
S_p	= spectral density of sound pressure in the interior
t	= time
w,w_1,w_2	= transverse panel displacements
X_{ijk}	= acoustic modes
x,y,z	= spatial coordinates
Z_{ij}	= defined by Eq. (17)
β	= structural damping coefficient
β_2	= loss factor of the viscoelastic damping tape material
ζ_{mn}	= panel modal damping coefficient
ζ^T_{mn}	= total modal damping coefficient (panel plus damping tape)
ζ_{ijk}	= acoustic modal damping coefficients
θ_{ijk}	= defined by Eqs. (33a) and (33b)
ν	= Poisson's ratio
ν_p	= Poisson's ratio for Plexiglass
ρ	= air density
ρ_s	= plate material density
ρ_p	= Plexiglas material density
ρ_T	= damping tape material density
Θ_{ij}	= defined by Eq. (15)
$\psi(z)$	= defined by Eq. (32)
χ_{mn}	= panel modes
ω	= frequency, rad/s
ω_{ijk}	= acoustic modal frequencies
ω_{mn}	= panel modal frequencies

Superscripts

—	= Fourier Transform

Presented as Paper 78-197 at the AIAA 16th Aerospace Sciences Meeting, Huntsville, Ala., Jan. 16-18, 1978; submitted March 3, 1978; revision received April 30, 1979.

Index categories: Cabin Environment, Crew Training, and Life Support; General Aviation; Noise.

*Associate Professor of Civil Engineering. Member AIAA.

I. Introduction

THE problem of predicting noise transmission into aircraft cabin is an essential field of study for interior noise control. The information available in the literature and from ongoing research programs indicates that noise in many aircraft exceeds acceptable comfort limits. This is especially evident for propeller-driven aircraft where maximum noise intensity occurs at low frequencies. Since acoustic absorption materials used in aircraft constructions are not very effective in reducing interior noise at low frequencies, other means of providing noise attenuation at these frequencies need to be established.[1]

A considerable interest on noise transmission by vibrating elastic surfaces has been shown in the past few years.[1-10] However, many of these investigations are directed to particular problems and it is difficult to generalize and apply these models for noise transmission into the aircraft. The objective of this paper is to construct an analytical model capable of predicting noise transmission into a light twin-engine G/A aircraft. The sidewalls of this type of aircraft are composed of many individual panels which are stiffened by stringers and frames as shown in Fig. 1. A more detailed description on structural and geometric parameters of this aircraft can be found in Ref. 11. The exact dynamic analysis of such sidewalls is too complicated, and a simplified model needs to be constructed. The vibrating surface is divided into several subpanel units (each unit is composed of one or more panels) for which the motions are taken to be independent. The total noise pressure inside the cabin is determined from the superposition of the contributions from each unit. The validity of this assumption depends on the degree of input pressure spatial correlations, the type of boundary supports of individual panels, and the significance of acoustic-structural mode coupling. Preliminary acceleration measurements tend to indicate that such an assumption is valid.[12]

The noise transmission into the aircraft is analyzed by solving the linear acoustic wave equation for the interior noise field and the plate vibration equation for the sidewall panel vibrations. The acoustic equation is coupled to panel vibrations through the time-dependent boundary conditions. The solution to this system of equations is obtained by using modal expansions and a Galerkin-type procedure. Since the boundary conditions for these equations are time-dependent, the commonly used method of separation of variables cannot be applied to this system.[13,14] The time dependence, however, is removed by splitting the solution into two parts: a solution corresponding to a nonhomogeneous differential equation with homogeneous boundary conditions and a solution on the boundary. Following this procedure, a uniformly convergent Fourier series solution is developed which converges rapidly not only in the interior acoustic space but also on the boundary.

This paper contains numerical results for the aircraft shown in Fig. 1 for which the exterior noise surface pressure inputs were measured.[12] Utilizing these inputs, the interior noise pressures in the cabin were calculated and compared to the available experimental data.[12] The effect on noise transmission due to stiffening, addition of damping, and mass is investigated. The results include narrow band, one-third octave, and overall noise pressure levels in the cabin.

II. Interior Acoustic Pressure

Consider the interior space of the aircraft shown in Fig. 1 to be approximated by a rectangular enclosure occupying a volume $V = abd$ as shown in Fig. 2. It is assumed that the main contribution to the interior noise comes from vibrating sidewalls at $z = 0,d$ (shown by a dashed line in Fig. 1), and that the remaining surfaces are acoustically rigid. Due to construction details and the location of input pressure sources (propellers and engine exhaust) in relation to the flexible sidewall, such an assumption seems to be justified. Taking the perturbation pressure p to be at rest prior to the motions of the flexible sidewalls, the pressure inside the enclosure with acoustically hard walls can be determined from the linear

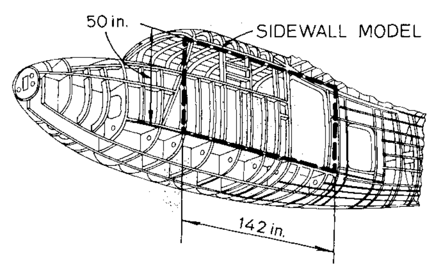

Fig. 1 Structural features of a twin-engine aircraft used for interior noise study.

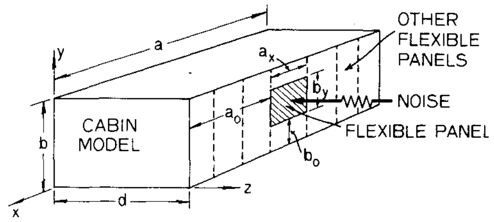

Fig. 2 Interior noise prediction model.

acoustic wave equation

$$\nabla^2 p = 1/c^2 \ddot{p} + Q \tag{1}$$

where ∇^2 is the Laplacian operator

$$\partial^2/\partial x^2 + \partial^2/\partial y^2 + \partial^2/\partial z^2$$

The boundary conditions to be satisfied are

$$\partial p/\partial n = 0 \text{ on } S_R \tag{2}$$

$$\partial p/\partial n = -\rho \ddot{w} \text{ on } S_F \tag{3}$$

where S_R and S_F indicate rigid and flexible boundaries, respectively, $\partial p/\partial n$ is the normal derivative to the wall surface; and w is the flexible wall displacement. The forcing term Q includes direct noise leakage into the cabin and/or the noise generated in the interior by some means other than the transmitted noise through the sidewalls.

By specifying the initial conditions on the flexible wall displacement w, the solution to Eq. (1) can be developed in time domain. Assuming that the random noise excitation has operated for a sufficiently long time and that the effects of initial conditions have died out, the solution to Eq. (1) can be obtained in frequency domain. Taking the Fourier Transformation of Eqs. (1-3) and writing the solution for pressure in terms of orthogonal eigenfunctions gives

$$\bar{p}(x,y,z,\omega) = \sum_{i=0}^{\infty} \sum_{j=0}^{\infty} \bar{P}_{ij}(z,\omega) X_{ij0}(x,y) \tag{4}$$

where

$$X_{ijk} = \cos\frac{i\pi x}{a} \cos\frac{j\pi y}{b} \cos\frac{k\pi z}{d} \qquad k = 0,1,2... \tag{5}$$

are the eigenfunctions of a rectangular cavity with hard walls, and a bar indicates the Fourier Transformation. Let the wall displacements at $z = 0,d$ be represented by $w_1(x,y,t)$ and $w_2(x,y,t)$, respectively. Expanding these flexible wall motions in terms of the acoustic cavity eigenfunctions given in Eq. (5), substituting Eq. (4) into Eqs. (1-3), and using orthogonality, we obtain

$$\mathrm{d}^2\bar{P}_{ij}/\mathrm{d}z^2 + [(\omega^2/c^2) - A_{ij}]\bar{P}_{ij} = \bar{Q}_{ij} \tag{6}$$

$$\mathrm{d}\bar{P}_{ij}/\mathrm{d}z = \bar{G}_{ij} \text{ at } z = 0 \tag{7}$$

$$\mathrm{d}\bar{P}_{ij}/\mathrm{d}z = \bar{E}_{ij} \text{ at } z = d \tag{8}$$

where

$$A_{ij} = (i\pi/a)^2 + (j\pi/b)^2 \tag{9}$$

$$\bar{Q}_{ij} = (e_{ij}/ab) \int_0^a \int_0^b \bar{Q} X_{ij0} \mathrm{d}x\mathrm{d}y \tag{10}$$

$$\bar{G}_{ij} = (e_{ij}\omega^2/ab) \int_{S_{F_1}} \int \rho \bar{w}_1 X_{ij0} \mathrm{d}x\mathrm{d}y \tag{11}$$

$$\bar{E}_{ij} = (e_{ij}\omega^2/ab)\int_{S_{F_2}}\int \rho\bar{w}_2 X_{ij0}\mathrm{d}x\mathrm{d}y \tag{12}$$

$$e_{ij} = \begin{cases} 1 & i=0,\ j=0 \\ 2 & \text{either } i\neq 0 \text{ or } j\neq 0 \\ 4 & i\neq 0,\ j\neq 0 \end{cases} \tag{13}$$

in which S_{F_1} and S_{F_2} indicate the flexible surface areas on the sidewalls at $z=0$ and $z=d$, respectively.

The solution to Eq. (6) with boundary conditions specified in Eqs. (7) and (8) and $Q=0$ can be written as

$$\bar{P}_{ij} = \Theta_{ij} + \bar{Z}_{ij}(z,\omega) \tag{14}$$

where Θ_{ij} are the solutions of the homogeneous boundary value problem

$$\bar{\Theta}_{ij} = \sum_{k=0}^{\infty} \bar{B}_{ijk}\cos k\pi z/d \tag{15}$$

and $\bar{Z}_{ij}$ are the solutions on the boundary. Since $\bar{\Theta}_{ij}$ are the solutions with homogeneous boundary conditions, $\mathrm{d}\bar{\Theta}_{ij}/\mathrm{d}z=0$ at $z=0,d$, from Eqs. (7, 8, and 14),

$$\mathrm{d}\bar{Z}_{ij}/\mathrm{d}z = \bar{G}_{ij} \quad \text{at } z=0 \tag{16a}$$

$$\mathrm{d}\bar{Z}_{ij}/\mathrm{d}z = \bar{E}_{ij} \quad \text{at } z=d \tag{16b}$$

A function which satisfies these boundary conditions is a polynomial of the form[14]

$$\bar{Z}_{ij} = \bar{G}_{ij}z + [(\bar{E}_{ij}-\bar{G}_{ij})/2d]z^2 \tag{17}$$

It should be noted that any continuous function which satisfies Eqs. (16a) and (16b) is a suitable function for $\bar{Z}_{ij}$. Substitution of Eq. (14) into Eq. (6) and utilization of the orthogonality principle gives

$$\bar{B}_{ijk} = H_{ijk}\bar{F}_{ijk} \tag{18}$$

where

$$H_{ijk} = 1/(\omega_{ijk}^2 - \omega^2 + 2\underline{i}\zeta_{ijk}\omega_{ijk}\omega) \tag{19}$$

$$\bar{F}_{ijk} = \frac{c^2 e_k}{d}\int_0^d \left\{\left(A_{ij}-\frac{\omega^2}{c^2}\right)\bar{Z}_{ij} - \frac{\mathrm{d}^2\bar{Z}_{ij}}{\mathrm{d}z^2}\right\}\cos\frac{k\pi z}{d}\mathrm{d}z \tag{20}$$

$$e_k = \begin{cases} 1 & k=0 \\ 2 & k\neq 0 \end{cases} \tag{21}$$

in which the "equivalent" acoustic damping was introduced through the modal damping coefficient ζ_{ijk}, and ω_{ijk} are the acoustic modal frequencies

$$\omega_{ijk} = \pi c\{(i/a)^2 + (j/b)^2 + (k/d)^2\}^{1/2} \tag{22}$$

The solution for sound pressure distribution inside the cabin is determined by combining Eqs. (4, 14, and 15):

$$\bar{p}(x,y,\omega) = \sum_{i=0}^{\infty}\sum_{j=0}^{\infty}\sum_{k=0}^{\infty}\bar{B}_{ijk}X_{ijk} + \sum_{i=0}^{\infty}\sum_{j=0}^{\infty}\bar{Z}_{ij}(z,\omega)X_{ij0} \tag{23}$$

Since F_{ijk} are functions of the sidewall response $\bar{w}_1$ and $\bar{w}_2$, next we determine the response of the flexible elastic panels.

III. Response of Sidewall Panels

The flexible portion of the sidewalls of the aircraft shown in Fig. 1 is composed of the load-bearing external skin which is stiffened by the stringers and frames, thermal and acoustic insulation, and the interior trim. For the purpose of this study it is assumed that the vibrations of individual panels are independent and that noise is transmitted by these panels directly into the aircraft interior with no effects from the trim.

The governing equation of motion for a panel located on the sidewall at $z=0$ or $z=d$ can be written in frequency domain as

$$D\nabla^4\bar{w} + \underline{i}\omega\beta\bar{w} - \rho_s h\omega^2\bar{w} = \bar{p}^r - \bar{p}|_{z=z^*} \tag{24}$$

where $\nabla^4 = \partial^4/\partial x^4 + 2\partial^4/\partial x^2\partial y^2 + \partial^4/\partial y^4$, $\bar{p}^r$ is the random external surface pressure due to propeller and engine noise or turbulent boundary layer, and $\bar{p}$ is the interior pressure given in Eq. (23) at $z^*=0$ or $z^*=d$. In obtaining Eq. (24), it was assumed that the effects on panel response by pressurization, panel curvature, surface flow aerodynamics, and in-plane loading can be neglected. The subscripts on deflection $\bar{w}$ have been dropped for brevity since the governing equations for panels located on the two sidewalls at $z=0$ and $z=d$ are similar and only material, input, and geometric parameters need to be adjusted.

The solution for the panel deflection $\bar{w}$ is expressed in terms of plate modes

$$w(x,y,\omega) = \sum_{m=1}^{\infty}\sum_{n=1}^{\infty}\bar{q}_{mn}(\omega)\chi_{mn}(x,y) \tag{25}$$

where $\bar{q}_{mn}$ are the generalized coordinates and χ_{mn} are panel modes. In this analysis, panels are taken to be clamped on all four edges for which the beam characteristic functions are utilized to obtain χ_{mn}.[15] Following the Galerkin method, we substitute Eq. (25) into Eq. (24), multiply by an orthogonal eigenfunction χ_{mn}, and integrate over the panel surface. The result is

$$\bar{q}_{mn} = H_{mn}(\bar{P}_{mn}^r - \bar{P}_{mn}^c) \tag{26}$$

where the panel frequency response function is

$$H_{mn} = 1/(\omega_{mn}^2 - \omega^2 + 2\underline{i}\zeta_{mn}\omega_{mn}\omega) \tag{27}$$

and the generalized forces are

$$\bar{P}_{mn}^r = \frac{1}{M_{mn}}\int_{a_0}^{a_0+a_x}\int_{b_0}^{b_0+b_y}\bar{p}^r(x,y,\omega)\chi_{mn}\mathrm{d}x\mathrm{d}y \tag{28}$$

$$\bar{P}_{mn}^c = \frac{1}{M_{mn}}\int_{a_0}^{a_0+a_x}\int_{b_0}^{b_0+b_y}\bar{p}(x,y,z^*,\omega)\chi_{mn}\mathrm{d}x\mathrm{d}y \tag{29}$$

in which the generalized mass is

$$M_{mn} = \rho_s h\int_{a_0}^{a_0+a_x}\int_{b_0}^{b_0+b_y}\chi_{mn}^2\mathrm{d}x\mathrm{d}y \tag{30}$$

The generalized coordinates $\bar{q}_{mn}$ are coupled through the generalized cavity pressure $\bar{P}_{mn}^c$. It has been observed in Refs. 6, 9, and 16 that cavity pressure effects on panel response are important for shallow cavities only. For cavity sizes corresponding to the light aircraft interior dimensions, cavity pressure effects might be important only for the fundamental panel mode. Under this assumption, the equations of motion uncouple.

IV. Acoustic-Structural Model

The equations for $\bar{p}$ and $\bar{w}$ developed in previous sections can be combined to construct a noise transmission model for light aircraft. From Eqs. (23) and (25) it can be shown that the interior acoustic pressure $\bar{p}$ due to vibrating panel at $z=0$ is

$$\bar{p}(x,y,z,\omega)=\frac{\rho\omega^2c^2}{ab}\sum_{i=0}^{\infty}\sum_{j=0}^{\infty}\sum_{k=0}^{\infty}e_{ij}[\theta_{ijk}H_{ijk}+e_k\psi(z)]\sum_{m=1}\sum_{n=1}L_{ijmn}H_{mn}\bar{P}^r_{mn}X_{ijk} \tag{31}$$

where

$$\psi(z)=z-z^2/2d \tag{32}$$

$$\theta_{ij0}=d/3\{-\omega^2/c^2+3/d^2+A_{ij}\},k=0 \tag{33a}$$

$$\theta_{ijk}=-\frac{d}{2(\pi k)^2}\{-\omega^2/c^2+A_{ij}\},k\neq 0 \tag{33b}$$

$$L_{ijmn}=\int_{a_0}^{a_0+a_x}\int_{b_0}^{b_0+by}X_{ij0}X_{mn}\mathrm{d}x\mathrm{d}y \tag{34}$$

Similar expressions can be developed for panels located on the sidewall at $z=d$. The total interior sound pressure is then determined by the superposition of the contributions by all panels from each sidewall. The interior pressure spectral density can be obtained by taking mathematical expectation of Eq. (31).[17] A more detailed treatment on the development of cavity pressure due to vibration of elastic panels is given in Refs. 18 and 19.

V. Numerical Results

The numerical results presented in this paper correspond to the aircraft shown in Fig. 1. It was assumed that noise enters by the airborne path only through the sidewalls with no leakage or noise generated directly in the cabin. The noise-transmitting sidewalls for this aircraft are composed of many individual panels which range in dimensions from about 6×15 in. (15×38 cm) to 10.5×27.5 in. (27×70 cm) and thickness from 0.032 to 0.064 in. (0.081 cm to 0.162 cm). It was assumed that each sidewall was composed of 16 flexible panels including 3 windows. The dimensions and thicknesses of each panel were estimated from the geometries suggested by the manufacturer. The windows are double-wall Plexiglas. For the analysis the windows were assumed to be made from a single sheet with a thickness of 0.14 in. (0.356 cm). The input noise pressure acting on each individual panel was assumed to be fully correlated over the panel surface. These inputs were taken from experimental measurements performed on this aircraft during static ground tests with both engines running at equal power input.

The numerical calculations were obtained for a constant structural damping ratio in all modes $\zeta_{mn}=0.02$ and acoustic damping ratio of the form

$$\zeta_{ijk}=0.03(\omega^l/\omega_{ijk}) \tag{35}$$

where ω^l is the lowest acoustic modal frequency in the cabin and ω_{ijk} are the acoustic modal frequencies given by Eq. (29). The following physical data were used in the computation: $a=142$ in. (361 cm), $b=50$ in. (127 cm), $d=48$ in. (122 cm), $c=1128$ fps (344 cm/s), $E=10^7$ psi (6.9×10^7 kN/m^2), $E_P/E=0.04$, $\rho_s=0.1\times h$ lb/in.^{2} ($0.69\times h$ kN/m^2), $\rho_p/\rho_s=0.416$, $\nu=0.3$, $\nu_p=0.35$, $\rho=0.002378$ slugs/cu. ft (1.225 kg/m^3), $x^*=35$ in. (89 cm), $y^*=35$ in. (89 cm), $z^*=12$ in. (30 cm).

The sound pressure levels in the interior were calculated from

$$\mathrm{SPL}(x^*,y^*,z^*,f)=10\log S_p(x^*,y^*,z^*,f)/p_0^2 \tag{36}$$

where SPL is expressed in decibels and p_0 is the reference pressure $p_0=2.9\times10^{-9}$ dyn/cm. In Fig. 3, interior sound levels are plotted vs frequency utilizing Eq. (36) and experimental measurements given in Ref. 12. The analytical results are obtained for surface densities of 0.77 lb/ft^2 (36.88 N/m^2) and 1.54 lb/ft^2 (73.77 N/m^2). Surface density of 0.77 lb/ft^2 corresponds to bare panels with no mass addition from stringers, frames, insulation, trim, paint, etc. Surface density of 1.54 lb/ft^2 might be a more realistic representation of an actual built-up sidewall. As can be observed from these results, the major peaks in the interior sound spectra occur at the propeller blade passage harmonics and the engine firing harmonics. Some of these peaks are intensified by the sidewall panel resonances. No significant peaks were observed at the acoustic cabin resonances.

Since the cabin noise levels for this aircraft are very high, a parametric study was performed on the effects of various sidewall treatments to reduce interior noise. These treatments include stiffening, addition of mass, and addition of damping. For all these cases, interior noise pressures were calculated using a narrow band analysis (2 Hz bands). From

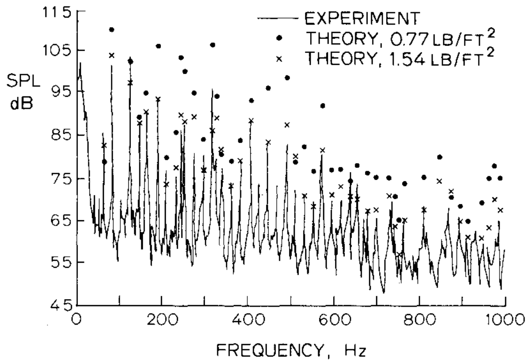

Fig. 3 Interior sound pressure levels at 2600 rpm.

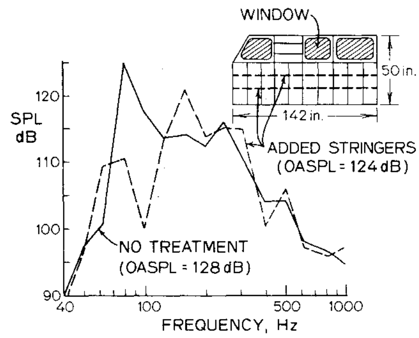

Fig. 4 Sound pressure in the cabin with two stringers attached to each sidewall.

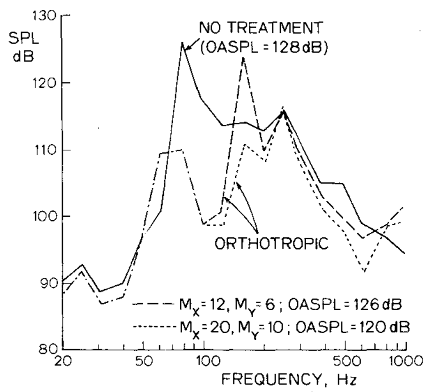

Fig. 5 Sound pressure in the cabin with orthotropic sidewalls.

these results, one-third octave and the overall noise levels were determined.

The effect on interior noise due to aircraft sidewall stiffening is illustrated in Figs. 4 and 5. The results given in Fig. 4 correspond to the case where two additional stiffeners were attached to each sidewall of the aircraft. It was assumed that these stiffeners provide clamped boundary conditions to individual panels and that the motions of individual panels are independent. The results indicate that this kind of stiffening would increase interior noise at most frequencies above 100 Hz. In Fig. 5 the results are presented for a case where a large number of stiffeners were attached to each sidewall. In this case the effect of stiffening was "smeared" to obtain an equivalent orthotropic panel model. The dynamic and the material properties of added stiffeners were chosen to be identical to the stiffeners now attached on the aircraft. Orthotropic panel natural frequencies corresponding to clamped-clamped boundaries were calculated from the approximate formulas given in Ref. 15. The results tend to indicate that this kind of stiffening of the aircraft sidewalls could have only a modest effect on interior noise reduction. It was found that for certain orthotropic stiffening configurations the interior noise could be amplified at some frequencies.

The effect on noise reduction due to addition of mass to one sidewall of the aircraft is shown in Fig. 6. As can be observed from these results, doubling the panel mass increases noise reduction by about 6 dB at higher frequencies. At low frequencies (below 100 Hz), mass addition tends to shift the fundamental panel frequencies to lower values thus shifting the peaks in noise reduction to the left.

Two types of damping were considered in the study. In the first case it was assumed that damping tape is attached to all panels on both sidewalls. The total damping coefficient (panel + damping tape) was calculated from approximate formula given in Ref. 8.

$$\zeta_{mn}^{T} = \zeta_{mn} + \frac{\beta_2 e_2 h_2 (3 + 6h_2 + 4h_2^2)}{2e_2 h_2 (3 + 6h_2 + 4h_2^2) + 1} \tag{37}$$

where $e_2 = E_2/E$ is the ratio of moduli of elasticity, $h_2 = h_T/h$ is the ratio of damping tape and panel thicknesses, ζ_{mn} are the modal damping coefficients of the panel, and β_2 is the

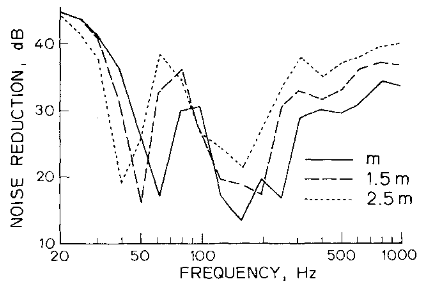

Fig. 6 Noise reduction for a sidewall with added mass.

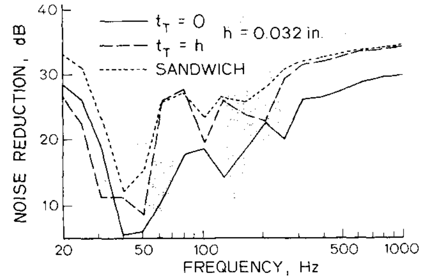

Fig. 7 Noise reduction for a sidewall with constrained and unconstrained damping treatments.

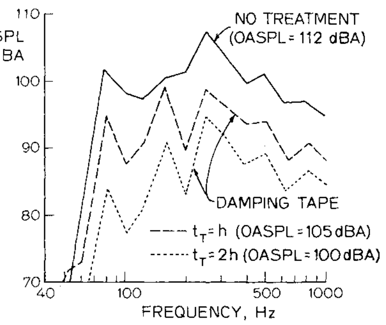

Fig. 8 A-weighted interior sound pressure levels with damping tape treatments.

loss factor of the viscoelastic damping tape material. In the second case it was assumed that a viscoelastic material with loss factor β_2 and shear modulus G is sandwiched between two elastic panels. This type of damping treatment is known as constrained layer damping. A detailed study on noise transmission by sandwich panels can be found in Ref. 19. In Fig. 7, noise reduction is plotted for a case where $h_2 = 1$, $e_2 = 0.01$, $\beta_2 = 0.5$, $G = 400$ psi (2.76×10^6 N/m^2), and $\rho_T/\rho_s = 0.8$.

It should be noted that when this kind of damping treatment is applied, mass is also added to the structure. These results tend to indicate that significant amount of noise reduction can be achieved by these damping treatments. In obtaining these results, it was assumed that damping treatment was applied to all panels including windows. The windows taken were rectangular in shape, flat, and clamped on all edges.

In Fig. 8, theoretically calculated interior noise due to measured inputs during a static ground test is shown for several damping tape configurations on an A-weighted scale. Overall noise levels are also indicated in this figure.

VI. Concluding Remarks

An analytical study was conducted to determine noise transmission characteristics into a light twin-engine G/A aircraft. The main emphasis was placed on evaluating the effect of noise transmission due to various add-on treatments. The results indicate that interior noise is strongly controlled by forced response due to propeller blade passage harmonics and engine firing harmonics. Interior noise amplification due to panel resonant vibrations was observed only at a few frequencies with no significant amplification from the acoustic cavity resonances. These observations correspond to 2600 rpm.

Stiffening of aircraft sidewalls does not seem to be an effective tool in reducing interior noise. Increased stiffness shifts modal frequencies to higher values, thus increasing noise on A-weighted scale. However, absorptive acoustic materials might be utilized more efficiently at higher frequencies to control interior noise. This study indicates that a combination of added mass and damping treatments to all panel surfaces including windows is the most effective mean in reducing interior noise for this aircraft in the low-frequency region. It should be noted that added mass will have some negative effect on aircraft performance and fuel efficiency, even though the percentage of added weight for noise control is very small in comparison to the gross weight of the aircraft.

Most of the present commercial, commuter, and G/A aircraft carry some additional weight solely for noise reduction treatments. Preliminary studies indicate that in the case of the new proposed fuel efficient turboprop aircraft (prop-fan propulsion units), a substantial amount of weight will need to be added in order to reach acceptable noise levels in the cabin. Perhaps a combination of stiffening, damping tape treatments, efficient use of absorptive materials, and redesign of nonload carrying items in the aircraft interior for lower weight will prove to be the best solutions for controlling noise in G/A aircraft for least amount of added weight. These conclusions are based on the results obtained under static conditions. In flight, due to forward speed effects, additional noise is transmitted from turbulent boundary layer. However, propeller noise inputs tend to decrease substantially in magnitude at higher frequency blade harmonics with increasing forward speed.

Acknowledgment

The author wishes to express his gratitude to Langley Research Center, Aircraft Noise Reduction Division, NASA, for their encouragement and financial support in preparing this paper, and to W. McDonald for contributions in computer program preparation.

References

[1]Cockburn, J.A. and Jolly, A.C., "Structural-Acoustic Response Noise Transmission Losses and Interior Noise Levels of an Aircraft Fuselage Excited by Random Pressure Fields," Tech. Rept. AFFDL-TR-68-2, U. S. Air Force, Aug. 1968.

[2]Lyon, R., "Noise Reduction of Rectangular Enclosures with One Flexible Wall," *Journal of the Acoustical Society of America*, Vol. 35, Nov. 1973, pp. 1791-1797.

[3]Kihlman, T., "Sound Radiation into a Rectangular Room. Application to Sound Transmission in Buildings," *Acustica*, Vol. 18, 1967, pp. 11-20.

[4]Strawderman, W.A., "The Acoustic Field in a Closed Space Behind a Rectangular Simply Supported Plate Excited by Boundary Layer Turbulence," Underwater Sound Laboratory Rept. 827, May 11, 1967.

[5]Bhattacharya, M.C. and Crocker, M.J., "Forced Vibration of a Panel and Radiation of Sound into a Room," *Acustica*, Vol. 22, 1969/1970, pp. 273-294.

[6]Guy, R.W. and Bhattacharya, M.C., "The Transmission of Sound Through a Cavity Backed Finite Plate," *Journal of Sound and Vibration*, Vol. 27, 1973, pp. 207-223.

[7]Wilby, J.F. and Scharton, T.D., "Acoustic Transmission Through a Fuselage Sidewall," BBN Rept. 2742, July 1974.

[8]Beranek, Leo L., ed., *Noise and Vibration Control*, McGraw-Hill, New York, 1971.

[9]Dowell, E.H., Gorman, G.F., III, and Smith, D.A., "Acoustoelasticity: General Theory Acoustic Natural Modes and Forced Response to Sinusoidal Excitation, Including Comparisons with Experiment," *Journal of Sound and Vibration*, Vol. 52, 1977, pp. 519-592.

[10]Koval, L.R., "On Sound Transmission into a Thin Cylindrical Shell Under Flight," *Journal of Sound and Vibration*, Vol. 48, 1976.

[11]Mixson, J.S., Barton, C.K., and Vaicaitis, R., "Investigation of Interior Noise in a Twin-Engine Light Aircraft," *Journal of Aircraft*, Vol. 15, April 1978, pp. 227-233.

[12]Barton, C.K. and Mixson, J.S., private communication. Langley Research Center, Aircraft Noise Reduction Division, NASA, 1976-1977.

[13]Courant, R. and Hilbert, D., *Methods of Mathematical Physics*, Vol. I, Interscience Publishers, 1953, pp. 277-281.

[14]Mindlin, R.D. and Goodman, L.E., "Beam Vibrations with Time Dependent Boundary Conditions," *Journal of Applied Mechanics*, Vol. 17, Dec. 1950, pp. 377-380.

[15]Rudder, F.F., Jr., and Plumblee, M.E., Jr., "Sonic Fatigue Design Guide for Military Aircraft," Air Force Flight Dynamics Laboratory, Wright-Patterson Air Force Base, Ohio, AFFDL-TR-74-112, May 1975.

[16]Dowell, E.H. and Voss, H.M., "The Effect of a Cavity on Panel Vibrations," *AIAA Journal*, Vol. 1, 1963, pp. 476-477.

[17]Lin, Y.K., *Probabilistic Theory of Structural Dynamics*, McGraw-Hill, New York, 1967, pp. 203-217.

[18]McDonald, W.B., Vaicaitis, R., and Myers, M.K., "Noise Transmission Through Plates into an Enclosure," NASA TP-1173, Langley Research Center, Hampton, Va., May 1978.

[19]Vaicaitis, R., "Noise Transmission by Viscoelastic Sandwich Panels," NASA TND-8516, Langley Research Center, August 1977.